







Article

Deactivation of a Vanadium-Based SCR Catalyst Used in a Biogas-Powered Euro VI Heavy-Duty Engine Installation

Johanna Englund ^{1,*} , Sandra Dahlin ² , Andreas Schaefer ¹ , Kunpeng Xie ³ ,
Lennart Andersson ³, Soran Shwan ³, Per-Anders Carlsson ¹ , Lars J. Pettersson ²
and Magnus Skoglundh ¹ 

¹ Competence Centre for Catalysis, Department of Chemistry and Chemical Engineering, Chalmers University of Technology, 412 96 Gothenburg, Sweden; andreas.schaefer@chalmers.se (A.S.); per-anders.carlsson@chalmers.se (P.-A.C.); skoglund@chalmers.se (M.S.)

² Department of Chemical Engineering, KTH Royal Institute of Technology, 114 28 Stockholm, Sweden; sanj@kth.se (S.D.); lpet@kth.se (L.J.P.)

³ Volvo Group Trucks Technology, 412 58 Gothenburg, Sweden; kunpeng.xie@volvo.com (K.X.); lennart.la.andersson@volvo.com (L.A.); soran.shwan@volvo.com (S.S.)

* Correspondence: johanna.englund@chalmers.se; Tel.: +46-31-772-2925

Received: 21 April 2020; Accepted: 14 May 2020; Published: 16 May 2020



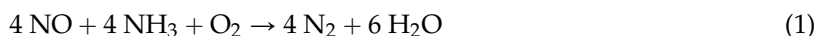
Abstract: We have investigated how the exhaust gases from a heavy-duty Euro VI engine, powered with biogas impact a vanadium-based selective catalytic reduction (SCR) catalyst in terms of performance. A full Euro VI emission control system was used and the accumulation of catalyst poisons from the combustion was investigated for the up-stream particulate filter as well as the SCR catalyst. The NO_x reduction performance in terms of standard, fast and NO₂-rich SCR was evaluated before and after exposure to exhaust from a biogas-powered engine for 900 h. The SCR catalyst retains a significant part of its activity towards NO_x reduction after exposure to biogas exhaust, likely due to capture of catalyst poisons on the up-stream components where the deactivation of the oxidation catalyst is especially profound. At lower temperatures some deactivation of the first part of the SCR catalyst was observed which could be explained by a considerably higher surface V⁴⁺/V⁵⁺ ratio for this sample compared to the other samples. The higher value indicates that the reoxidation of V⁴⁺ to V⁵⁺ is partially hindered, blocking the redox cycle for parts of the active sites.

Keywords: NH₃-SCR; V₂O₅-WO₃/TiO₂; catalyst deactivation; biogas; methane; engine-bench

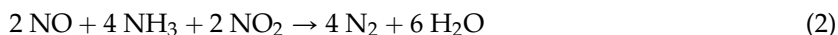
1. Introduction

The combination of decreased carbon dioxide (CO₂) and nitrogen oxides (NO_x) emissions in recent legislation for heavy-duty vehicles puts a large pressure on the efficiency and durability of the emission control system [1]. The performance of one of the last parts of the emission control system of a heavy-duty vehicle, the selective catalytic reduction (SCR) catalyst which reduces NO_x to N₂, is of major importance as well as the particulate filter (DPF) which reduces the emissions of particulate matter (PM). The limit for NO_x emissions from a heavy-duty vehicle in the present standard in Europe, Euro VI, is set to 0.4 g/kWh (World Harmonized Stationary Cycle, WHSC). This standard also contains limits for emissions of PM, carbon monoxide (CO), hydrocarbons (HC) and ammonia slip, and the emissions need to comply to set limits throughout the lifetime of the vehicle, which is seven years or 700,000 km whichever occurs first [2]. Due to the recent inclusion of limits for CO₂ emissions or greenhouse gas (GHG) equivalents, new approaches are needed for engine and emission control. Engines with higher fuel-efficiency will reduce CO₂ emissions, however this

will also lead to a reduction of the exhaust temperature, which will make it difficult for the emission control system to perform efficiently [3]. Another approach is to move from using fossil based fuels to more sustainable non-fossil fuels like biodiesel and biogas. This will not decrease the amount of CO₂ that is emitted from the vehicle but it will move the emissions from fossil carbon towards bio-based carbon. One potential complication from using bio-based fuels is the presence of catalyst poisons such as sulfur (S), phosphorus (P) and alkali metals, which can reduce the activity as well as the selectivity of the catalysts [4,5]. A common way to reduce NO_x to N₂ is by using an SCR catalyst in combination with a reducing agent. The most commonly used reducing agent in heavy-duty vehicles is urea, which decomposes and hydrolyses to NH₃ in the exhaust stream at temperatures above 180 °C [6]. The SCR reaction can proceed through three different routes: the standard, fast and NO₂ SCR reaction route shown in Equations (1)–(3), respectively [7].



An oxidation catalyst (DOC) is usually placed up-stream of the SCR catalyst and the DPF, and this catalyst oxidizes NO to NO₂. The ratio between NO₂ and NO dictates which route the SCR reaction mainly follows. When the ratio is around 1 the reaction follows the fast SCR reaction route (Equation (2)).



In NO₂ excess, NO₂ can be reduced to N₂ according to the NO₂-rich route (Equation (3)).



One of the most commonly used SCR catalysts in heavy-duty vehicles is V₂O₅-WO₃ supported on TiO₂. The advantage with this catalyst compared to the other commonly used SCR catalyst, Cu-SSZ-13, is that the vanadium-based catalyst is robust towards sulfur poisoning [8–11]. However, its low-temperature performance is lower compared to that of Cu-SSZ-13. Nevertheless an up-stream oxidation catalyst that converts NO to NO₂ to achieve fast SCR conditions could overcome this gap in performance. Deactivation of the vanadium-based catalyst has been extensively studied [4,12–15]. It has been shown by Blakeman et al. that the amount of sulfur in the feed is a significant parameter where a low concentration of sulfur could benefit the SCR reaction, while a high concentration could cause severe but reversible deactivation of the catalyst [16,17]. The presence of alkali metals and zinc in the fuel, and lube oil can cause severe permanent deactivation by impacting the Brønsted acid sites resulting in a decrease in the adsorption of ammonia, which is an important step in the SCR reactions [13–15,18]. When the catalyst is subjected to phosphorus some activity is lost, but most studies found that the deactivation is not proportional to the amount of phosphorus adsorbed on the catalyst. The observed deactivation is lower than expected, and this is likely due to the acidic nature of phosphorus [12,19,20]. It is also most likely due to this acidity, which provides ammonia adsorption sites, that phosphorus could decrease the negative impact on the catalyst caused by alkali compounds. Many of the studies performed have been on single poisons or by impregnating the catalyst with poisons which are quite far from real conditions. Nevertheless, these studies provide valuable input into mechanisms and reaction paths for the deactivation, but full system investigations, using the real fuel in an engine, also needs to be performed.

In the present study, aging of a vanadium-based SCR catalyst after exposure to exhaust-gases from a heavy-duty (Euro VI) engine powered with biogas during 900 h has been investigated. The exhaust after-treatment system is a full Euro VI system. In this way the impact on the SCR catalyst from using biogas as fuel can be evaluated in a real-life exhaust environment.

2. Results and Discussion

After exposing the SCR catalyst samples (described in Table 1) to exhaust from a biogas-powered engine in an engine-bench for 900 h, the performance of these samples in terms of SCR activity was evaluated. The SCR performance was evaluated for three different reaction conditions; standard, fast and NO₂-rich SCR. The results for these experiments are presented in Figures 1–3, respectively. The activity was evaluated at steady state conditions at six different temperature points. Between these points the temperature was increased linearly at a rate of 10 °C/min. After 900 h of exposure to biogas exhaust, only a minor decrease in NO_x conversion during the standard SCR reaction is observed for the first SCR catalyst (SCR1) compared to the fresh sample (Figure 1). This decrease is observed for both the inlet and the outlet part of the catalyst, at temperatures below 300 °C. The measurable error in the measurements is small, +/−0.5 percentage at most, however, since the difference in conversion is minor it is important to be aware of the potential error in the measurement.

Table 1. Sample description and nomenclature.

Sample Name	Description
SCR fresh	Fresh sample of the SCR catalyst
SCR1 in	Inlet sample of the first consecutive engine-bench aged SCR catalyst
SCR1 out	Outlet sample of the first consecutive engine-bench aged SCR catalyst
SCR3 in	Inlet sample of the third and last consecutive engine-bench aged SCR catalyst
SCR3 out	Outlet sample of the third and last consecutive engine-bench aged SCR catalyst
DPF in	Inlet sample of the engine-bench aged DPF
DPF out	Outlet sample of the engine-bench aged DPF

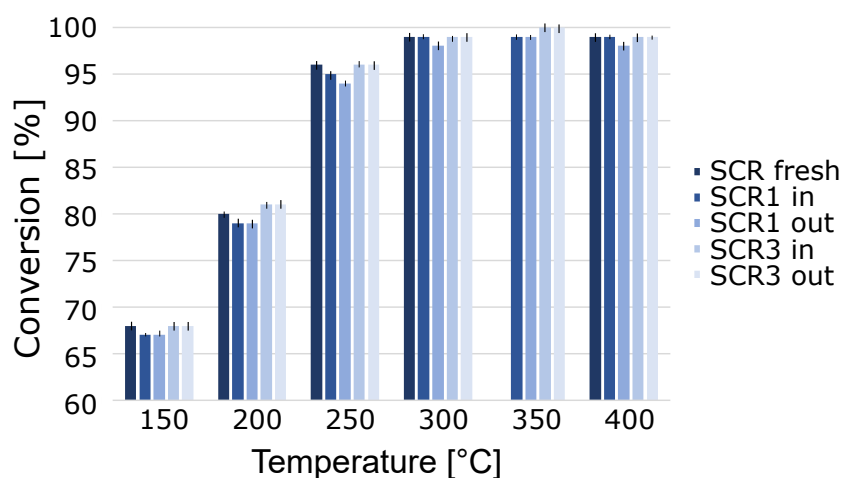


Figure 1. Conversion of NO_x over the fresh selective catalytic reduction (SCR) catalyst (SCR fresh), the inlet and outlet samples of SCR catalyst 1 (SCR1 in and SCR1 out, respectively) and the inlet and outlet samples of SCR catalyst 3 (SCR3 in and SCR3 out, respectively) at steady state for six temperatures, 150, 200, 250, 300, 350 and 400 °C at standard SCR conditions. The feed consisted of 1100 ppm NH₃, 1000 ppm NO, 8% O₂, 5% H₂O with argon as balance. The space velocity used was 45,000 h^{−1}.

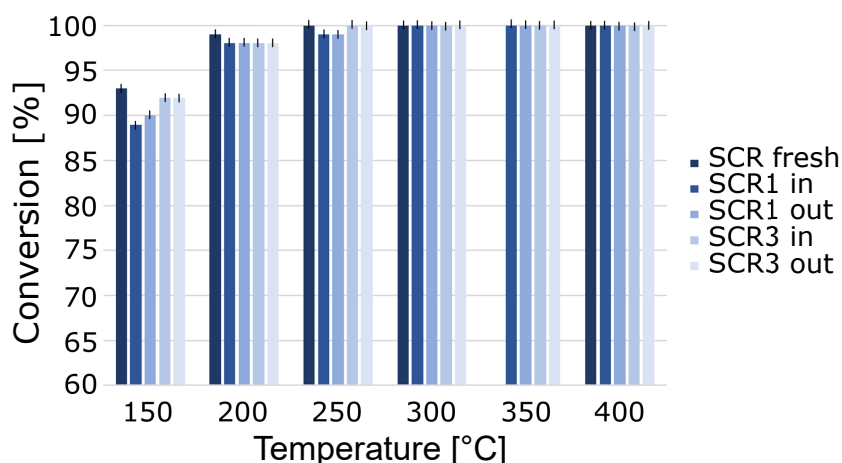


Figure 2. Conversion of NO_x over the fresh SCR catalyst (SCR fresh), the inlet and outlet samples of SCR catalyst 1 (SCR1 in and SCR1 out, respectively) and the inlet and outlet samples of SCR catalyst 3 (SCR3 in and SCR3 out, respectively) at steady state for six temperatures, 150, 200, 250, 300, 350 and 400 °C at fast SCR conditions. The feed consisted of 1100 ppm NH_3 , 500 ppm NO, 500 ppm NO_2 , 8% O_2 , 5% H_2O with argon as balance. The space velocity used was 45,000 h^{-1} .

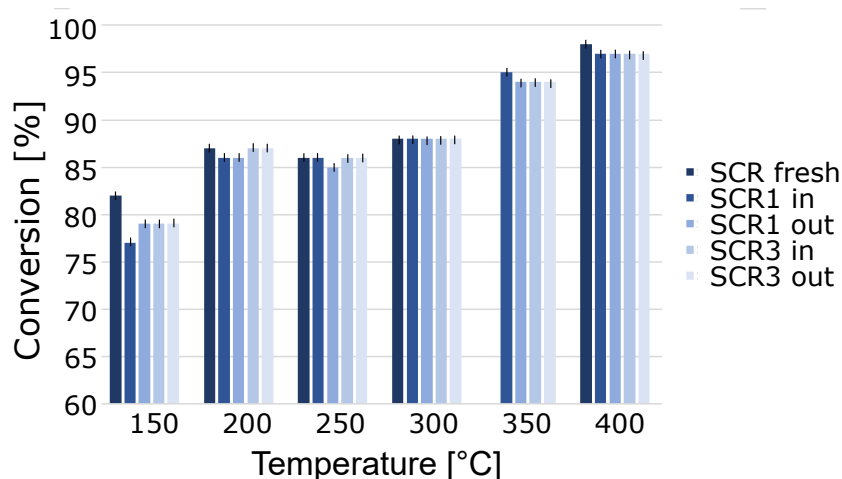


Figure 3. Conversion of NO_x over the fresh SCR catalyst (SCR fresh), the inlet and outlet samples of SCR catalyst 1 (SCR1 in and SCR1 out, respectively) and the inlet and outlet samples of SCR catalyst 3 (SCR3 in and SCR3 out, respectively) at steady state for six temperatures, 150, 200, 250, 300, 350 and 400 °C at NO_2 -rich SCR conditions. The feed consisted of 1100 ppm NH_3 , 250 ppm NO, 750 ppm NO_2 , 8% O_2 , 5% H_2O with argon as balance. The space velocity used was 45,000 h^{-1} .

Comparing the results from standard and fast SCR conditions, the overall conversion of NO_x is significantly higher for the latter reaction condition, and at 300 °C the conversion reaches 100% for all SCR samples. At lower temperatures though, a slight decrease in NO_x conversion for the SCR1 inlet and outlet samples can be seen (Figure 2).

When testing the catalyst samples under NO_2 -rich SCR conditions, the same pattern is observed as under fast and standard SCR conditions. The samples from the first SCR catalyst show a slightly higher degree of deactivation than the samples from the third SCR catalyst (Figure 3).

Even though the decrease in NO_x conversion is low, other changes to the catalysts could be observed after the 900 h exposure to biogas exhaust. For the experiments conducted with higher concentration of NO_2 in the feed, a slight increase in N_2O formation could be seen for the samples

originating from the first SCR catalyst (SCR1) at 400 °C. The formation of N₂O increased from close to zero to 5 ppm for both the inlet and the outlet sample of the first SCR catalyst after engine-bench aging.

From the NH₃-TPD experiments, another change was seen in the engine-bench aged samples. These samples have a decreased ability to adsorb NH₃, especially the outlet samples are impacted. As seen in Table 2, the outlet samples of the engine-bench aged catalysts lost 50% of their ammonia adsorption capacity while the inlet sample only lost 25 and 15%, respectively for SCR catalyst 1 and 3. This loss in NH₃ adsorption capacity is not reflected in the decrease in activity for the engine-bench aged samples. The decrease in NH₃ adsorption capacity for the outlet samples could be due to the slight increase of sulfur concentration in the outlet part of both catalyst samples as seen by X-ray fluorescence (XRF) measurements (PANalytical Epsilon 3XL) in Table 3. The outlet samples contain slightly higher concentrations of vanadium due to uneven coating which means that the decrease in NH₃ adsorption is not due to less vanadium on these samples. For the inlet sample of SCR catalyst 1, the temperature where maximum NH₃ desorption occurs (T_{max}) is shifted towards higher temperatures, while the remaining engine-bench aged samples have a T_{max} relatively close to that of the fresh SCR sample. This shift is likely part of the explanation to the slight decrease in activity for this sample at lower temperatures.

Table 2. Desorption of NH₃ during a heating ramp from 150 to 400 °C at a rate of 10 °C/min relative to the desorption for the SCR fresh sample. Temperature for maximum NH₃ desorption, T_{max} , is also presented. The feed during the heating ramp consisted of 5% H₂O in argon. Gas hourly space velocity (GHSV): 45,000 h⁻¹.

Sample	Desorbed Amount of NH ₃ [% of SCR Fresh]	T_{max} [°C]
SCR fresh	100	236
SCR1 in	76	253
SCR1 out	48	229
SCR3 in	87	238
SCR3 out	48	226

Table 3. Content of P, S, Ca and Zn in the fresh SCR catalyst (SCR fresh), the inlet and outlet samples of SCR catalyst 1 (SCR1 in and SCR1 out, respectively), the inlet and outlet samples of SCR catalyst 3 (SCR3 in and SCR3 out, respectively), the inlet and outlet samples of the particulate filter (DPF in and DPF out, respectively), the fresh oxidation catalyst (DOC fresh) and the inlet and outlet samples of oxidation catalyst (DOC in and DOC out, respectively) as obtained by XRF analysis. * The binder used when preparing the samples for XRF analysis contains 82 ppm phosphorus. ** Results for the DOC samples are published in reference [21].

Sample	Phosphorus [%]	Sulfur [ppm]	Calcium [ppm]	Zinc [ppm]
SCR fresh	0.19 *	400	1.7	-
SCR1 in	0.17 *	630	1.5	-
SCR1 out	0.20 *	820	1.6	-
SCR3 in	0.18 *	650	1.5	-
SCR3 out	0.18 *	840	1.6	-
DPF in	0.06 *	890	380	160
DPF out	0.09 *	1300	1000	480
DOC fresh **	0.00	0	280	-
DOC in **	0.18	2700	470	-
DOC out **	0.04	2500	320	-

Ammonia does not only participate in the SCR reactions, under certain circumstances the ammonia could be undesirably oxidized by O_2 to N_2 and H_2O which is not desired. Below $300\text{ }^\circ\text{C}$ the vanadium-based SCR catalyst used in this study shows no activity towards ammonia oxidation during NH_3 oxidation conditions. However at $350\text{ }^\circ\text{C}$, some oxidation of ammonia occurs as can be seen in Figure 4, where the conversion of ammonia in the presence of oxygen and water is presented. The ammonia is oxidized into N_2 and H_2O at temperatures up to $400\text{ }^\circ\text{C}$, which is the maximum temperature the engine-bench aged samples are tested at to avoid any regeneration during testing. At temperatures above $400\text{ }^\circ\text{C}$, the fresh SCR catalyst also starts to convert some NH_3 to N_2O , NO and NO_2 .

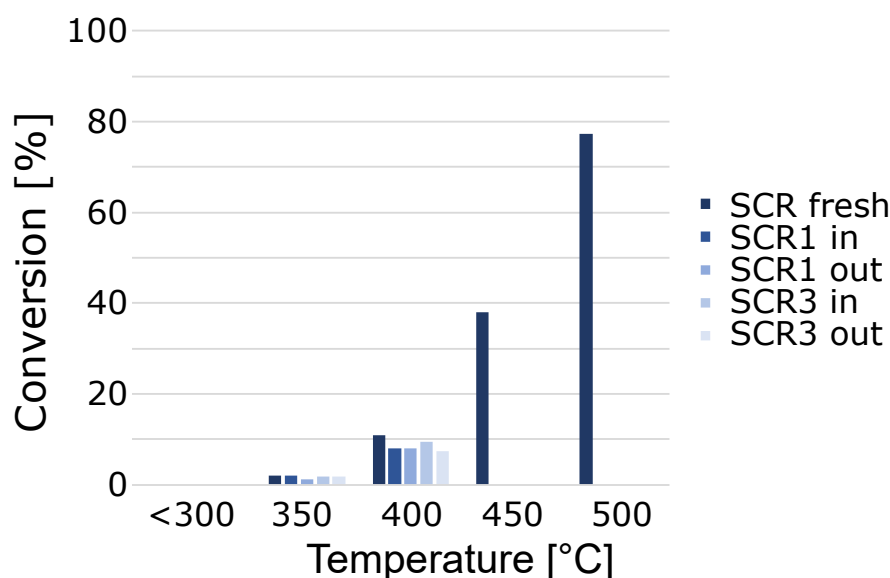


Figure 4. Conversion of NH_3 over the fresh SCR catalyst (SCR fresh), the inlet and outlet samples of SCR catalyst 1 (SCR1 in and SCR1 out, respectively) and the inlet and outlet samples of SCR catalyst 3 (SCR3 in and SCR3 out, respectively) at steady state for five temperatures, 200, 250, 300, 350 and $400\text{ }^\circ\text{C}$ at NH_3 oxidation conditions. The SCR fresh sample was also measured at 450 and $500\text{ }^\circ\text{C}$. The feed consisted of 1000 ppm NH_3 , 8% O_2 , 5% H_2O with argon as balance. The space velocity used was $45,000\text{ h}^{-1}$.

Up-stream of the SCR catalysts, an oxidation catalyst and a particulate filter are placed. These emission control components will partially capture catalyst poisons from the exhaust gas, which means that the gas feed that enters the first SCR catalyst is relatively clean from contaminants such as sulfur and phosphorus. Data for the oxidation catalyst have recently been published [21], showing that the majority of the phosphorus in the biogas exhaust ends up on the inlet part of the oxidation catalyst which indicates that it adsorbs on the first surface it comes in contact with. Most of the phosphorus sticks in the form of P_2O_5 or phosphorus glass, however, small amounts of phosphorus will continue to the particulate filter and downstream components of the emission control system. However, sulfur is not as likely to mainly adsorb on the inlet part of the oxidation catalyst, but is rather distributed evenly over the length of the oxidation catalyst. Sulfur will, to a larger extent, continue to the emission control system components downstream the oxidation catalyst. To try to elucidate where in the emission control system the catalyst poisons end up, the particulate filter as well as the SCR catalyst samples were analyzed by X-ray fluorescence (XRF) spectrometry, see Table 3. The data published for the oxidation catalyst [21] shows that high concentrations of phosphorus are found in the inlet part of the catalyst (DOC in) while lower amounts are found in the outlet part (DOC out). For the next consecutive component of the emission control system, the particulate filter, it can be seen in Table 3 that some phosphorus has accumulated as well as some sulfur. Higher concentrations

of poisons are observed in the outlet part of the DPF compared to the inlet part, as opposed to what was observed for the DOC. This is due to the design of the particulate filter, which is a wall-flow filter with alternately plugged channels, in the inlet and outlet part of it, causing accumulation of ash, particulate matter and poisons mainly on the outlet part of the filter. The accumulation of poisons on the DOC and the DPF is, however, not only beneficial for the performance the SCR catalyst since the deactivation of these components will cause a decrease in NO_2/NO_x ratio [21], which in turns leads to a decreased capacity for NO_x reduction in the SCR catalyst [22].

The results from the XRF analysis show that no significant amounts of phosphorus or calcium are accumulated in the samples of the SCR catalyst after engine-bench aging for 900 h using biogas as fuel. Sulfur is found in slightly higher amounts on the engine-bench aged samples and then in particular in the outlet samples, which could explain the significant decrease in NH_3 storage capacity for these samples, see Table 2.

The X-ray photoelectron spectroscopy (XPS) measurements of a small section of the SCR samples do not show a significant amount of phosphorus on the surface. The P 2p signal visible in Figure S1 in the supplementary material is not changing in intensity for the different samples. No sulfur signal is detected for any of the samples, which is the opposite to the XRF results. The S 2p signal is likely below the detection limit because XPS is a highly surface sensitive technique compared to XRF, which probes the whole sample.

Detailed spectra of the vanadium 2p region are compiled in Figure 5. The V 2p_{3/2} peaks are deconvoluted into two components centered around 517.1 ± 0.1 eV and 515.9 ± 0.1 eV. Based on the binding energy positions the components are assigned to V^{5+} in V_2O_5 (higher binding energy) and V^{4+} in VO_2 (lower binding energy) [23]. The ratio of the V^{4+} and V^{5+} signal with respect to the total V 2p signal (as shown in Figure 6) is fairly similar for all samples with the exception of the SCR1 in sample. For this sample the $\text{V}^{4+}/\text{V}^{5+}$ ratio is considerably higher when compared to the other samples. The higher ratio indicates that the reoxidation of V^{4+} to V^{5+} is partially hindered, blocking parts of the active sites and hence, causing the activity for NO_x reduction to decrease.

The O 1s spectra that are shown in the supplementary material exhibit two distinct components at 529.9 eV and at high/ V^{4+} er binding energy at about 532.3 eV. Oxygen 1s signals around 530 eV are found for most metal oxides while a signal around 532.4–533 eV is reported for SiO_2 [24], which is also part of the catalyst material in the present study. However, also the signal of OH groups that can form is located close to 532 eV for most metal oxide materials [25]. As seen in Figure S2, the outlet samples exhibit a higher intensity at about 532 eV which could be interpreted as a higher amount of OH groups present on the surface of those samples. However, a clear assignment of the oxide and OH-related signal is not possible due to the presence of various metal oxides in the samples (see further discussion in the supplementary material). Hence at this point we can only speculate that those additional OH groups may be another explanation of the reduced NH_3 adsorption capacity at the outlet parts of the SCR samples.

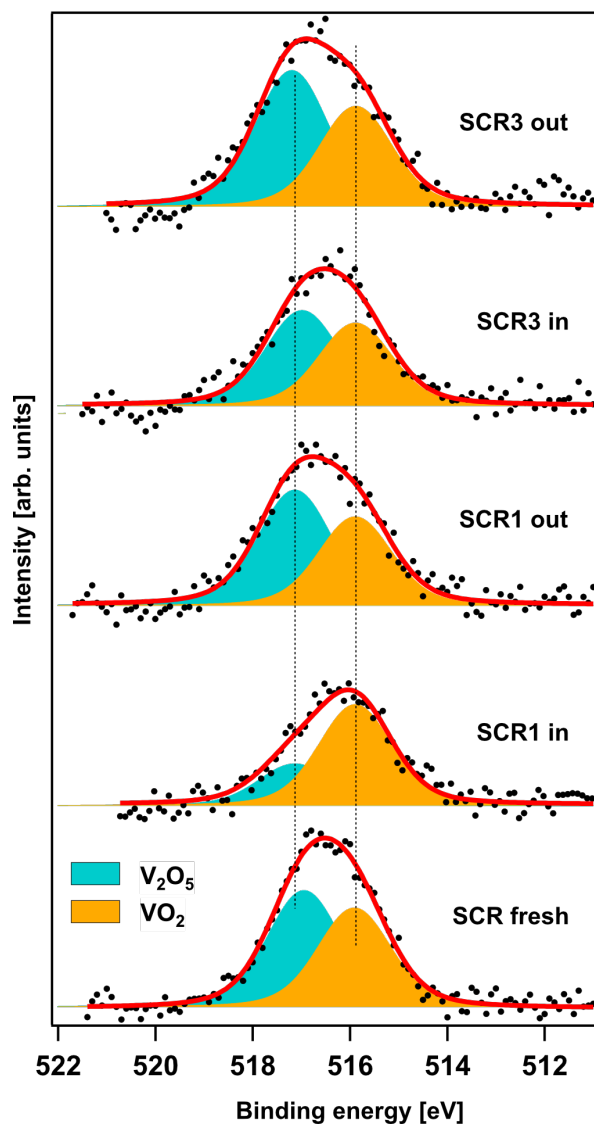


Figure 5. Vanadium $2p_{3/2}$ core level spectra of the fresh SCR catalyst and the inlet and outlet samples of SCR catalyst 1 and 3, respectively. Data points after background subtraction are shown as dots, the solid line represents the result of curve fitting by the two shaded components shown.

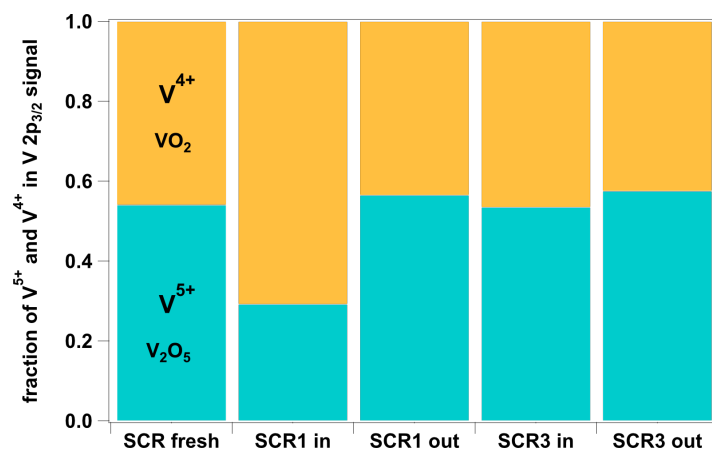


Figure 6. Fraction of V^{5+} and V^{4+} relative to the total $V 2p_{3/2}$ signal.

3. Materials and Methods

An engine-bench including a heavy-duty engine from Volvo (G13C 460 hp) and an Euro VI type emission control system (Volvo Group Trucks Technology, Gothenburg, Sweden) was used for aging the catalysts. The emission control system is shown schematically in Figure 7. The type of engine used is a dual-fuel type using 90% biogas and 10% diesel as fuel for a duration of 900 h. The aging corresponds to half a lifetime in temperature exposure and around 25–30% of a lifetime in terms of chemical exposure. The average sulfur content in biogas could be around 5 mg/m³ which gives a lifetime exposure of 300 g sulfur, which means that the exposure during the engine-bench aging is around 75–90 g of sulfur. The concentration of phosphorus in biogas is generally low and the contribution of phosphorus in the exhaust is assigned to the lubrication oil used in the engine. The gas flow to the engine was altered in cycles for the duration of the engine aging to replicate driving on roads. The inlet temperature of the first consecutive SCR catalyst during the engine-bench aging varied between 170 and 550 °C during the entire aging. After 900 h of engine-bench aging, each part of the emission control system was investigated separately.

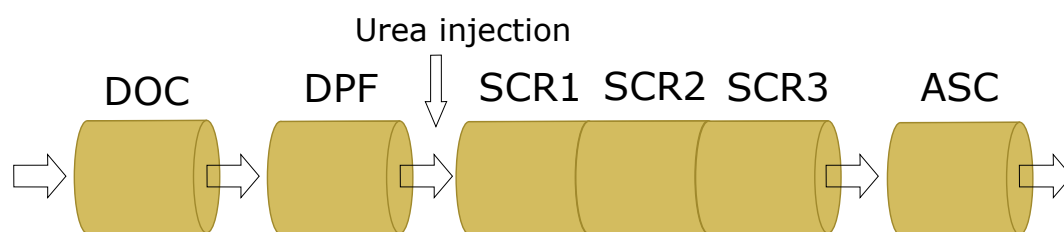


Figure 7. Emission control system set-up with the oxidation catalyst (DOC), particulate filter (DPF), SCR catalysts (SCR 1-3) and ammonia slip catalyst (ASC).

3.1. Catalyst Material

The NO_x reduction catalyst used in this study is a commercially available tungsten promoted vanadium-based V₂O₅-WO₃/TiO₂ SCR catalyst. From the catalysts used in the engine-bench aging, smaller sample cores were drilled out (11 mm diameter and 19 mm length). These smaller sample cores were used for the evaluation of catalyst performance in a synthetic gas bench and for catalyst characterization. The loading of vanadia in the sample, including support, was around 1–1.5 wt%, the tungsten loading was between 4 and 8 wt%, the cell density and geometry of the sample was 260 cpsi and the V₂O₅-WO₃ was impregnated on a fiberglass-reinforced TiO₂ substrate in a corrugated shape. Samples were obtained from the inlet and outlet parts of the first and last SCR catalyst to detect any differences over the length of the catalyst. The engine-bench aged SCR catalyst samples were compared with a fresh reference sample. The particulate filter used was a Pt/Pd supported on alumina type DPF. The DPF was only tested for catalyst poison content in this study and samples from both the inlet and outlet of the DPF were analyzed for content of P, S, Ca and Zn.

3.2. SCR Performance

A synthetic gas bench reactor (SGB, Chalmers University of Technology, Gothenburg, Sweden) was used to assess the catalyst performance in terms of standard, fast and NO₂-rich SCR. The experimental protocol is seen in Table 4. The SGB reactor, described elsewhere [26], consists of a horizontal quartz tube in a plane position heated by a resistive heating coil. Bronkhorst Hi-Tech mass flow controllers (Bronkhorst High-Tech B.V., Ruurlo, The Netherlands) were used to control the gas flow and the water feed was controlled by a Bronkhorst CEM system. The outlet gas concentrations from the SGB were analyzed by Fourier transform infrared spectrometry (FTIR) using an MKS 2030 HS device (MKS instruments, Andover, MA, USA). The temperature was controlled using a thermocouple located in a blank monolith up-stream the catalyst.

Table 4. Experimental protocol for activity tests. Base feed for all experiments except NH₃-TPD: 8 vol.-% O₂, 5 vol.-% H₂O with Ar used as balance. The space velocity used was 45,000 h⁻¹. The SCR steps were performed at 150, 200, 250, 300 and 400 °C, the NH₃ oxidation at 200, 250, 300, 350 and 400 °C while the NH₃-TPD was performed during a temperature ramp from the exposure temperature 150 °C to 400 °C at a heating rate of 10 °C/min. The fresh SCR sample was tested up to 500 °C but to avoid regeneration of the engine-bench aged samples they were only evaluated up to 400 °C except during TPD when the temperature went o 500 °C for all samples.

Step	NO [vol.-ppm]	NO ₂ [vol.-ppm]	NH ₃ [vol.-ppm]	Description
1	1000	-	1100	Standard SCR
2	500	500	1100	Fast SCR
3	250	750	1100	NO ₂ -rich SCR
4	-	-	1000	NH ₃ oxidation
5	-	-	-	Cooling to 150 °C in pure argon
6	-	-	400	NH ₃ adsorption for TPD
7	-	-	-	Argon flush
8	-	-	-	NH ₃ desorption at a heating rate of 10 °C/min to 500 °C

3.3. Characterization

To analyze if the NH₃ oxidation activity of the SCR catalyst changed after 900 h in the engine-bench, NH₃-oxidation tests were performed. This experiment was performed in the same gas bench reactor as the SCR performance tests and the experimental protocol can be seen in Table 4.

To quantify the NH₃ adsorption capacity of the catalysts, temperature-programmed desorption (TPD) of NH₃ was conducted according to the second part of the experimental protocol in Table 4.

X-ray fluorescence spectrometry was performed using a PANalytical Epsilon 3XL analyzer (Malvern Panalytical B.V., Almelo, The Netherlands) to semi-quantatively determine the elemental composition of the fresh and engine-bench aged SCR catalyst samples as well as samples from the DPf. Around 2 g of each of the samples were used for the analysis and the catalyst material as well as the fiberglass-reinforced TiO₂ substrate was analyzed. A ball mill was used to mix the samples with a binder (300 rpm, 10 min) and this mixture was pressed into flat discs (150 kN, 3 min).

X-ray photoelectron spectroscopy was employed to obtain information about the chemical state at the very surface of the samples. The spectrometer (VersaProbe III Scanning XPS Microprobe, Physical Electronics, Chanhassen, MN, USA) houses a monochromatized Al K_α radiation source (1486.6 eV). As a result that the samples were not electrically conductive, an electron neutralizer and an ion gun (Ar⁺) were used to compensate for charging effects. Preparation of the samples was performed by first cutting pieces from the catalyst sample and then fixing them to the sample holder with carbon tape. The samples were dried under vacuum over night at room temperature to desorb the majority of water. The area scanned with by XPS was about 500 × 500 μm². Based on the inelastic mean free path of the photoelectrons, an information depth of about 5 nm is estimated. The carbon 1s spectrum located at 284.5 eV [27] was used to calibrate the binding energy scale. The V 2p spectra shown in Figure 5 were normalized to the intensity on the low binding energy side. The spectra were then deconvoluted using a symmetric Doniach-Šunjić (DS) line profile with a DS half width of 0.5 eV [28] convoluted with a Gaussian whose half width was allowed to vary between 1.65 and 1.9 eV. A Shirley type background was subtracted prior to fitting.

4. Conclusions

Exposure to biogas exhaust for a duration of 900 h in an engine-bench set-up has only minor impact of the NO_x reduction ability for the vanadium-based SCR catalyst. Compared to the fresh catalyst sample a small decrease in activity for the NO_x reduction in fast, standard and NO₂-rich SCR conditions at temperatures below 300 °C was observed for the engine-bench aged samples, in particular for the samples taken from the SCR catalyst located at the furthest up-stream position. A likely explanation for the low degree of deactivation of the SCR catalysts is that the catalyst poisons present in the engine exhaust mainly stick to the up-stream parts of the emission control system, primarily the oxidation catalyst, but also the particulate filter, where higher concentrations of P, S and Ca were found using XRF, SEM-EDX and XPS. Even if the effect of biogas exhaust exposure on the SCR activity was minor, other changes to the SCR catalysts were observed. The ability of the SCR catalyst to adsorb NH₃ decreased considerably after exposure to biogas exhaust, where the outlet samples were particularly impacted. This could be explained by a more significant accumulation of sulfur on the outlet parts of the SCR catalysts. The deactivation observed for the inlet sample of the first SCR catalyst could be explained by the shift in V⁴⁺/V⁵⁺ ratio, which was seen for this sample using XPS. The ratio was considerably higher for the inlet sample of the first SCR catalyst when compared to the other samples indicating that the reoxidation of V⁴⁺ to V⁵⁺ is partially hindered, blocking the redox cycle for parts of the active sites hence, causing the activity for NO_x reduction to decrease. The importance of addressing the deactivation of the entire emission control system becomes clear in this study. Since the deactivation of the SCR catalyst itself is not severe one could assume that the amount of NO_x emitted from the system is low. This is not the case though, especially at low temperatures where the deactivation of the up-stream oxidation catalyst causes a decrease in NO₂ formation which results in an overall lower NO_x conversion in the SCR catalyst hence, increased emission of NO_x.

Supplementary Materials: The following are available online at <http://www.mdpi.com/2073-4344/10/5/552/s1>, Figure S1: Fraction of XPS survey spectra, Figure S2: Oxygen and silicon region of XPS spectra, S3: Titanium and vanadium region of XPS spectra, S4: Tungsten region of XPS spectra.

Author Contributions: Conceptualization, L.J.P. and M.S.; data curation, J.E., S.D. and A.S.; formal analysis, J.E., A.S., L.J.P. and M.S.; funding acquisition, L.J.P. and M.S.; investigation, J.E. and A.S.; methodology, J.E., A.S., K.X., L.A., S.S., L.J.P. and M.S.; project administration, J.E. and S.D.; resources, S.D., A.S., K.X., L.A. and S.S.; supervision, L.A., P.-A.C., L.J.P. and M.S.; visualization, J.E.; writing—original draft, J.E.; writing—review and editing, J.E. All authors have read and agreed to the published version of the manuscript.

Funding: This work was financially supported by the Swedish Energy Agency through the FFI program (No: 38364-1) and the Competence Centre for Catalysis, which is financially supported by Chalmers University of Technology, the Swedish Energy Agency, and the member companies AB Volvo, ECAPS AB, Johnson Matthey AB, Preem AB, Scania CV AB, Umicore Denmark ApS, and Volvo Car Corporation AB.

Conflicts of Interest: The authors declare no conflict of interest.

References

1. Regulation (EU) 2019/631. Official Journal of the European Union: Brussels, 2019. Available online: <https://eur-lex.europa.eu/legal-content/EN/TXT/?uri=CELEX%3A32019R0631> (accessed on 13 May 2020).
2. Regulations No 595/2009; Official Journal of the European Union: Brussels, 2009. Available online: <https://eur-lex.europa.eu/eli/reg/2009/595/oj> (accessed on 13 May 2020).
3. Binder, A.J.; Toops, T.J.; Unocic, R.R.; Parks, J.E., II; Dai, S. Low-Temperature CO Oxidation over a Ternary Oxide Catalyst with High Resistance to Hydrocarbon Inhibition. *Angew. Chem. Int. Ed.* **2015**, *54*, 13263–13267. [[CrossRef](#)] [[PubMed](#)]
4. Dahlin, S.; Nilsson, M.; Bäckström, D.; Bergman, S.L.; Bengtsson, E.; Bernasek, S.L.; Pettersson, L.J. Multivariate analysis of the effect of biodiesel-derived contaminants on V₂O₅-WO₃/TiO₂ SCR catalysts. *Appl. Catal. B Environ.* **2016**, *183*, 377–385. [[CrossRef](#)]
5. Chiodo, V.; Maisano, S.; Zafarana, G.; Urbani, F. Effect of pollutants on biogas steam reforming. *Int. J. Hydrog. Energy* **2017**, *42*, 1622–1628. [[CrossRef](#)]

6. Koebel, M.; Strutz, E.O. Thermal and Hydrolytic Decomposition of Urea for Automotive Selective Catalytic Reduction Systems: Thermochemical and Practical Aspects. *Ind. Eng. Chem. Res.* **2003**, *42*, 2093–2100. [[CrossRef](#)]
7. Devadas, M.; Kröcher, O.; Elsener, M.; Wokaun, A.; Söger, N.; Pfeifer, M.; Demel, Y.; Mussmann, L. Influence of NO₂ on the selective catalytic reduction of NO with ammonia over Fe-ZSM5. *Appl. Catal. B Environ.* **2006**, *67*, 187–196. [[CrossRef](#)]
8. Hammershøi, P.S.; Jensen, A.D.; Janssens, T.V. Impact of SO₂-poisoning over the lifetime of a Cu-CHA catalyst for NH₃-SCR. *Appl. Catal. B Environ.* **2018**, *238*, 104–110. [[CrossRef](#)]
9. Hammershøi, P.S.; Jangjou, Y.; Epling, W.S.; Jensen, A.D.; Janssens, T.V. Reversible and irreversible deactivation of Cu-CHA NH₃-SCR catalysts by SO₂ and SO₃. *Appl. Catal. B Environ.* **2018**, *226*, 38–45. [[CrossRef](#)]
10. Lezcano-Gonzalez, I.; Deka, U.; van der Bij, H.; Paalanen, P.; Arstad, B.; Weckhuysen, B.; Beale, A. Chemical deactivation of Cu-SSZ-13 ammonia selective catalytic reduction (NH₃-SCR) systems. *Appl. Catal. B Environ.* **2014**, *154–155*, 339–349. [[CrossRef](#)]
11. Shan, Y.; Shi, X.; Yan, Z.; Liu, J.; Yu, Y.; He, H. Deactivation of Cu-SSZ-13 in the presence of SO₂ during hydrothermal aging. *Catal. Today* **2019**, *320*, 84–90. [[CrossRef](#)]
12. Kamata, H.; Takahashi, K.; Odenbrand, I. Surface acid property and its relation to SCR activity of phosphorus added to commercial V₂O₅(WO₃)/TiO₂ catalyst. *Catal. Lett.* **1998**, *53*, 65–71. doi:10.1002/0931117. [[CrossRef](#)]
13. Klimczak, M.; Kern, P.; Heinzelmann, T.; Lucas, M.; Claus, P. High-throughput study of the effects of inorganic additives and poisons on NH₃-SCR catalysts—Part I: V₂O₅-WO₃/TiO₂ catalysts. *Appl. Catal. B Environ.* **2010**, *95*, 39–47. [[CrossRef](#)]
14. Nicosia, D.; Czekaj, I.; Kröcher, O. Chemical deactivation of V₂O₅/WO₃-TiO₂ SCR catalysts by additives and impurities from fuels, lubrication oils and urea solution: Part II. Characterization study of the effect of alkali and alkaline earth metals. *Appl. Catal. B Environ.* **2008**, *77*, 228–236. [[CrossRef](#)]
15. Chen, L.; Li, J.; Ge, M. The poisoning effect of alkali metals doping over nanoV₂O₅-WO₃/TiO₂ catalysts on selective catalytic reduction of NO_x by NH₃. *Chem. Eng. J.* **2011**, *170*, 531–537. [[CrossRef](#)]
16. Blakeman, P.; Arnby, K.; Marsh, P.; Newman, C.; Smedler, G. Optimization of an SCR Catalyst System to Meet EU IV Heavy Duty Diesel Legislation. In Proceedings of the 2008 SAE International Powertrains, Fuels and Lubricants Congress, Berlin, Germany, 16–18 June 2008. [[CrossRef](#)]
17. Granstrand, J.; Dahlin, S.; Immele, O.; Schmalhorst, L.; Lantto, C.; Nilsson, M.; Paris, R.S.; Regali, F.; Pettersson, L.J. Catalytic aftertreatment systems for trucks fueled by biofuels—Aspects on the impact of fuel quality on catalyst deactivation. *RSC Catal.* **2018**, *30*, 64–145. [[CrossRef](#)]
18. Kröcher, O.; Elsener, M. Chemical deactivation of V₂O₅/WO₃-TiO₂ SCR catalysts by additives and impurities from fuels, lubrication oils, and urea solution: I. Catalytic studies. *Appl. Catal. B Environ.* **2008**, *77*, 215–227. [[CrossRef](#)]
19. Blanco, J.; Avila, P.; Barthelemy, C.; Bahamonde, A.; Odriozola, J.; Banda, J.G.D.L.; Heinemann, H. Influence of phosphorus in vanadium-containing catalysts for NO_x removal. *Appl. Catal.* **1989**, *55*, 151–164. [[CrossRef](#)]
20. Castellino, F.; Rasmussen, S.B.; Jensen, A.D.; Johnsson, J.E.; Fehrmann, R. Deactivation of vanadia-based commercial SCR catalysts by polyphosphoric acids. *Appl. Catal. B Environ.* **2008**, *83*, 110–122. [[CrossRef](#)]
21. Englund, J.; Xie, K.; Dahlin, S.; Schaefer, A.; Jing, D.; Shwan, S.; Andersson, L.; Carlsson, P.A.; Pettersson, L.J.; Skoglundh, M. Deactivation of a Pd/Pt Bimetallic Oxidation Catalyst Used in a Biogas-Powered Euro VI Heavy-Duty Engine Installation. *Catalysts* **2019**, *9*, 1014. [[CrossRef](#)]
22. Iojoiu, E.; Lauga, V.; Abboud, J.; Legros, G.; Bonnet, J.; Da Costa, P.; Schobing, J.; Brillard, A.; Leyssens, G.; Tschamber, V.; et al. Biofuel Impact on Diesel Engine After-Treatment: Deactivation Mechanisms and Soot Reactivity. *Emiss. Control Sci. Technol.* **2018**, *4*, 15–32. [[CrossRef](#)]
23. Silversmit, G.; Depla, D.; Poelman, H.; Marin, G.B.; De Gryse, R. Determination of the V2p XPS binding energies for different vanadium oxidation states (V⁵⁺ to V⁰⁺). *J. Electron Spectrosc. Relat. Phenom.* **2004**, *135*, 167–175. [[CrossRef](#)]
24. Wu, J.X.; Wang, Z.M.; Ma, M.S.; Li, S. X-ray photoemission studies of praseodymium thin films on SiO₂/Si(100). *J. Phys. Condens. Matter* **2003**, *15*, 5857–5864. [[CrossRef](#)]
25. Dupin, J.C.; Gonbeau, D.; Vinatier, P.; Lévassieur, A. Systematic XPS studies of metal oxides, hydroxides and peroxides. *Phys. Chem. Chem. Phys.* **2000**, *2*, 1319–1324. [[CrossRef](#)]

26. Kannisto, H.; Ingelsten, H.H.; Skoglundh, M. Ag-Al₂O₃ catalysts for lean NO_x reduction—Influence of preparation method and reductant. *J. Mol. Catal. A Chem.* **2009**, *302*, 86–96. [[CrossRef](#)]
27. Moulder, J.F.; Stickle, W.F.; E'Sobol, P.; Bomben, K.D. *Handbook of X-ray Photoelectron Spectroscopy*; Perkin-Elmer Corporation: Eden Prairie, MN, USA, 1992.
28. Campbell, J.L.; Papp, T. Widths of the Atomic K–N7 Levels. *At. Data Nucl. Data Tables* **2001**, *77*, 1–56. [[CrossRef](#)]



© 2020 by the authors. Licensee MDPI, Basel, Switzerland. This article is an open access article distributed under the terms and conditions of the Creative Commons Attribution (CC BY) license (<http://creativecommons.org/licenses/by/4.0/>).